Variation in error-based and reward-based human motor learning is related and associated with entorhinal volume

Anouk J. de Brouwer[1], Mohammad R. Rashid[2], J. Randall Flanagan[1,3], Jordan Poppenk[1,3], Jason P. Gallivan[1,3,4]

1 Centre for Neuroscience Studies, Queen's University, Kingston, ON, Canada
2 School of Computing, Queen's University, Kingston, ON, Canada
3 Department of Psychology, Queen's University, Kingston, ON, Canada
4 Department of Biomedical and Molecular Sciences, Queen's University, Kingston, ON, Canada

Corresponding author: Anouk J. de Brouwer (ajdebrouwer@gmail.com)

Abstract

Error-based and reward-based processes are critical for motor learning, and are thought to be supported via distinct neural pathways. However, recent behavioral work in humans suggests that both learning processes are supported by cognitive strategies and that these contribute to individual differences in motor learning ability. While it has been speculated that medial temporal lobe regions may support this strategic component to learning, direct evidence is lacking. Here we first show that faster and more complete learning during error-based visuomotor adaptation is associated with better learning during reward-based shaping of reaching movements. This result suggests that strategic processes, linked to faster and better learning, drive individual differences in both error-based and reward-based motor learning. We then show that right entorhinal cortex volume was larger in good learning individuals—classified across both motor learning tasks—compared to their poorer learning counterparts. This suggests that strategic processes underlying both error- and reward-based learning are linked to neuroanatomical differences in entorhinal cortex.

Keywords: motor adaptation, visuomotor rotation, explicit learning, reinforcement, individual differences

Significance Statement

While it is widely appreciated that humans vary greatly in their motor learning abilities, little is known about the processes and neuroanatomical bases that underlie these differences. Here, using a data-driven approach, we show that individual variability in error-based and reward-based motor learning is tightly linked, and related to the use of cognitive strategies. We further show that structural differences in entorhinal cortex predict this intersubject variability in motor learning, with larger entorhinal volumes being associated with better overall error-based and reward-based learning. Together, these findings provide support for the notion that the ability to recruit strategic processes underlies intersubject variability in both error-based and reward-based learning, which itself may be linked to structural differences in medial temporal cortex.

Introduction

The human brain's capacity to learn new motor commands is fundamental to almost all activities we engage in. It is not only essential when we acquire novel skills, such as learning to play a musical instrument, but is also required on a daily basis as we refine existing motor skills and adapt to changes in our environment. To date, the vast majority of studies on motor learning have focused on characterizing learning across individuals at the group-level, treating individual variability as noise that obscures the main processes underlying learning. More recently, however, there has been increased interest in the potential sources of such intersubject variability (1–4), as they may provide insight into the specific mechanisms by which different people learn. While a handful of studies have helped uncover several of these mechanisms (1, 5, 6), little is known about their underlying neuroanatomical basis.

Traditionally, motor learning has been viewed as an implicit, procedural process of the motor system, with neural studies focusing on brain areas in the frontoparietal cortex, striatum or cerebellum (7–9). The putative role of cognitive brain circuits in driving motor learning has often been neglected (though see 10). Ever since the classic finding that patient H.M. showed learning of a visuomotor skill despite a bilateral medial temporal lobectomy (11, 12), motor and cognitive brain circuits have been viewed as operating largely independently of one another. Only relatively recently have behavioral studies demonstrated the myriad ways in which cognitive systems support motor learning — showing, for example, that processes related to strategy use and declarative memory can bolster, or interfere with, aspects of motor learning (13–16).

When considering the neural bases of such interactions, it is important to distinguish between two main forms of learning. Error-based learning is the form of learning by which we refine and adjust our movements to changes in the body or the environment based on observable errors, such as when missing the bullseye in archery. Such learning is thought arise from two separate processes acting in parallel: An implicit process that is driven by the error between predicted and observed sensory feedback (17, 18) and an explicit process that is driven by the error between the target and the sensory feedback (i.e., the task error) (19). The implicit process is nonconscious (i.e., resistant to voluntary control), adapts and de-adapts gradually and is reliant on the cerebellum (20–22). The explicit process, by contrast, is declarative in nature, and linked to the use of cognitive strategies resulting in large, rapid changes during early learning (13, 23), such as when intentionally aiming the bow slightly to the left of the bulls eye when shooting in a strong wind. Recent evidence further suggests that, while the implicit component to learning is fairly stable across tasks and participants (24, 25), individual differences in the rate of learning largely reflects whether, and how effectively, a cognitive strategy is implemented (2, 3). To date, the neural systems associated with this explicit component of learning remain rather speculative. Evidence from neuroimaging, aging, and lesion studies have implicated areas in the prefrontal cortex in explicit strategies (7, 26–28). In addition, it has been speculated, but not yet shown, that regions in the MTL, given their role in declarative processes, may also be involved in the explicit component to motor learning (3, 7, 29).

Reward-based learning is the form of learning that underlies the acquisition of many motor skills, such as when learning to swing on a playground set or learning to drink from a straw. When learning such skills, the mapping between success (reward) and motor commands is often highly complex, with no single error providing information about the required change in motor commands. Thus, in such cases, the brain must figure out the motor commands that increase success, often through active exploration and exploitation of the acquired knowledge (30–32). The neural circuits that drive reward-based learning are thought to be different from those involved in error-based learning, and critically rely on the basal ganglia and striatum (8, 33, 34). However, recent behavioral work suggests a key role for explicit strategies in reward-based motor learning (35, 36) and there is some emerging evidence from human neuroimaging to suggest links between the MTL and reward-based learning (37, 38). Insofar as active motor exploration may involve the use of strategies, it is plausible that MTL structures also contribute to success in reward-based motor learning.

To date, the role of MTL regions in declarative memory and spatial navigation have been well established (39–42). In humans, for example, anatomical imaging methods have demonstrated clear links between individual differences in hippocampus and/or entorhinal cortex volume and performance in memory and navigation tasks (43–50). It is increasingly recognized, however, that the hippocampal-entorhinal system is not solely dedicated to declarative memory or spatial navigation processes per se, but can support more abstract relational representations (51–54). Influential theories posit that this system forms a flexible 'cognitive' map for representing goals and relating objects and actions within a spatial context (41, 55, 56). Such maps are likely to be critical when forming new action-outcome associations, as is the case when searching for and implementing strategies during motor learning. Extending this notion of a cognitive map, here we asked whether individual differences in performance during motor learning are linked to hippocampal and entorhinal volume in humans. To examine this, we had human participants undergo a structural neuroimaging session prior to performing separate error-based and reward-based learning tasks, both known to elicit the use of strategies during learning. We show that learning performance in both motor tasks is directly related and that faster and better overall learning across tasks is associated with larger entorhinal cortex volume.

Results

In order to determine the relationship between motor performance in reward-based and error-based learning tasks, and the extent to which the size of hippocampal and entorhinal cortex may be associated to such learning, we collected high-resolution structural MRI scans from participants (N=34) prior to performing two separate motor learning tasks outside the scanner. In the reward-based learning task, inspired by Dam and colleagues (57), participants learned to copy an invisible, curved path through trial and error, using only a score (between 0 and 100 points) to improve their performance. This score, presented at the end of each trial, indicated how closely the participants' drawn path corresponded to the invisible path (Fig. 1B). Participants drew these paths on a digital drawing tablet from a start to a target position displayed on a vertical monitor (Fig. 1A), and were instructed to maximize their score. To obtain a representative measure of each participant's reward-based learning rate and ability, we had participants perform this task for 12 different invisible paths, with 20 attempts for each. Participants were naive to the possible shapes of the paths, which were shaped as single curves (i.e., half sine waves) and double curves (i.e., full sine waves) between the start and target position, with different amplitudes (see Fig. 1C). Because participants received only visual feedback about their path trajectory—and never the

rewarded path—they did not receive error-based information that could be used to guide learning. By design, this reward-based task requires implementing a search strategy to first find the invisible path and then refine the drawn path, and we thus predict that participants who perform well in this task are better at implementing such strategies.

In the error-based learning task, we used the classic visuomotor rotation learning paradigm (58), wherein participants had to adjust their movements to a 45° rotation of the cursor movement, which represented participants' hand movements, in order to hit visual targets (Fig. 1D). Participants performed center-out reaching movements on the drawing tablet to one of eight targets displayed on a monitor. After a baseline phase with veridical cursor feedback, participants were exposed to the 45° visuomotor rotation of the movement of the cursor, requiring an adjustment of the reaching movement in the opposite direction. Learning in this task consists of two components: automatic, implicit adjustments of the reach direction, resulting in gradual changes in performance, and the implementation of an aiming strategy to counteract the rotation, resulting in fast changes in performance (19, 23). Our previous work has shown (3) — and we predict here — that faster and more complete learning across participants will be largely driven by the use of an aiming strategy, used to counteract the rotation. At the end of the first block of rotation trials, we assessed this aiming strategy by asking participants to report the intended aiming angle by turning a knob with their left hand to rotate a line on the screen at the start of the trial, before executing the reach (19). Learning was then 'washed out' by restoring veridical cursor feedback, after which the visuomotor rotation was re-instantiated to assess the rate of re-learning.

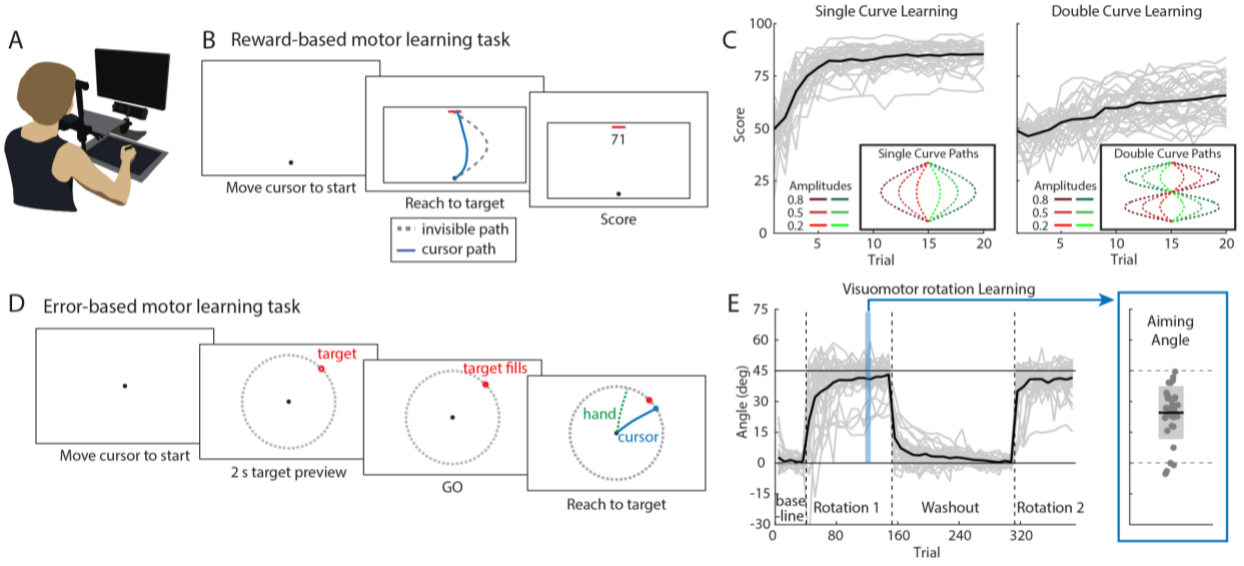

Figure 1. Experimental setup and task. (A) Setup. Participants made reaching movements by sliding a pen across a digitizing tablet without vision of the hand. The stimuli and a cursor representing the hand position were presented on a monitor. (B) Reward-based motor learning task. Participants were instructed to 'copy' an invisible path (dashed grey line), with a score between 0 and 100 indicating how close their drawn path (blue line) was to the hidden path. (C) Learning across trials for single (left panel) and double invisible paths (right panel). Each grey line is an individual participant (n=33), with the black line representing the average across participants. Insets depict the six single curve invisible paths and the six double curve invisible paths used in the task. (D) Error-based motor learning task. Participants made center-out reaching movements to visual targets (red dot) on a ring of landmarks (small grey dots) with veridical cursor feedback (not shown) or under a 45° rotation of the cursor feedback (blue line; hand direction is shown in green). (E) Learning curve (left panel) across the baseline, rotation 1, washout, and rotation 2 block, and reported aiming angle (right panel) measured at the end of the first rotation block. Each grey line or dot represents an individual participant (n=33), the black lines represent the mean across participants. The shaded grey area in the right panel represents the standard deviation.

Performance in reward-based and error-based motor learning is related

The black traces in Figure 1C and 1E show the learning curves, averaged across all participants, for the reward-based and error-based learning tasks, respectively. These figures demonstrate that participants learned to increase their scores in the reward-based task and change their hand angle in the error-based task across trials. However, these group-averaged results may be somewhat misleading, as they obscure significant intersubject variability in both the rates and levels of learning obtained (see gray traces in Fig. 1C,E, which depict single participants). For example, Figure 2 shows the behavior of two participants, one 'good' overall learner and one 'poor' overall learner, in both the reward-based learning task and the error-based learning task. Figure 2A and 2B depict the paths that the participants drew (left panel) and the corresponding scores (right panel), in two blocks of the reward-based learning task for a single (top) and double curve (bottom) with the largest amplitude (blocks 4 and 11 for the participant in Fig. 2A; blocks 11 and 10 for the participant in Fig. 2B). While both participants quickly converged on a good solution for the single curve, resulting in scores close to 100, the movements of the participant in Figure 2A resemble the invisible curve more closely. In addition, while the participant in Figure 2A quickly converges upon a solution that has a similar shape to the invisible double curve, the participant in Figure 2B never learns to draw that same double curve, and their score remains low.

Figure 2C and 2D show, for the same two participants, the median hand angle (in blue) for each bin of eight trials across the error-based learning task, as well as the reported aiming angle (in

purple) assessed near the end of the first rotation block. Appropriate corrections for the visuomotor rotation are plotted as positive values; that is, a hand angle of 45° corresponds to full compensation for the rotation. The participant in Figure 2C shows quick adjustment of the hand angle towards 45° in the first and second rotation block, and a quick return towards 0° in the washout block. Such fast learning is associated with a large contribution of an aiming strategy, consistent with their reported aiming angles around 39°. The participant in Figure 2D, by contrast, shows only gradual adjustments of the hand angle in the rotation and washout blocks, and correspondingly reports aiming values around 0°, suggesting that learning in this participant is mainly driven by the implicit process. Overall, the participant in Figure 2A,C showed better learning performance in both tasks than the participant in Figure 2B,D.

For each participant, we obtained six learning scores for the reward-based learning task (single and double curves × three amplitudes, positive and negative amplitudes were averaged) and seven learning scores for the error-based learning task (early and late learning in rotation block 1, washout, and rotation block 2, and the reported aiming angle). Across the entire group, we found significant correlations in the learning scores within and between the two tasks (Fig. 2E). To derive single participant measures of learning that capture these relationships across both tasks, and that can be used to relate learning to the neuroanatomical data collected in these same participants, we performed a principal component analysis (PCA) on the learning scores (see *Methods* for details). We found that the first (PC1) and second principal components (PC2) explained 42.4% and 13.4% of the variance in the data, respectively. The projection plots in Figure 2F allows for straightforward interpretation of these PCs, directly showing both the magnitude and sign of the loading of each of our 13 learning measures (six from the reward-based task and seven from the error-based task) onto PC1 and PC2. PC1 has positive loadings for all of the learning measures, indicating that this component captures overall learning performance. In other words, it provides a single measure that distinguishes between relatively 'good' and 'poor' learning performance in both the reward-based and error-based learning tasks. Indeed, PC1 shows significant positive correlations with all behavioral measures (ranging from r=0.37 to r=0.77, p=0.032 to p<0.001). The second principal component (PC2) broadly distinguishes between performance in the reward-based and error-based learning task, with positive loadings for the reward-based learning scores, negative loadings for learning in the rotation blocks, and little contribution of learning in the washout blocks. However, it explains only a small portion of the behavioral variance (13.4%), limiting the interpretational value of this component and its use in further analyses. Taken together, our approach demonstrates that performance in both tasks is

219 highly related; a single measure captures whether participants are good learners in the reward-
220 based learning and in the error-based learning task.
221

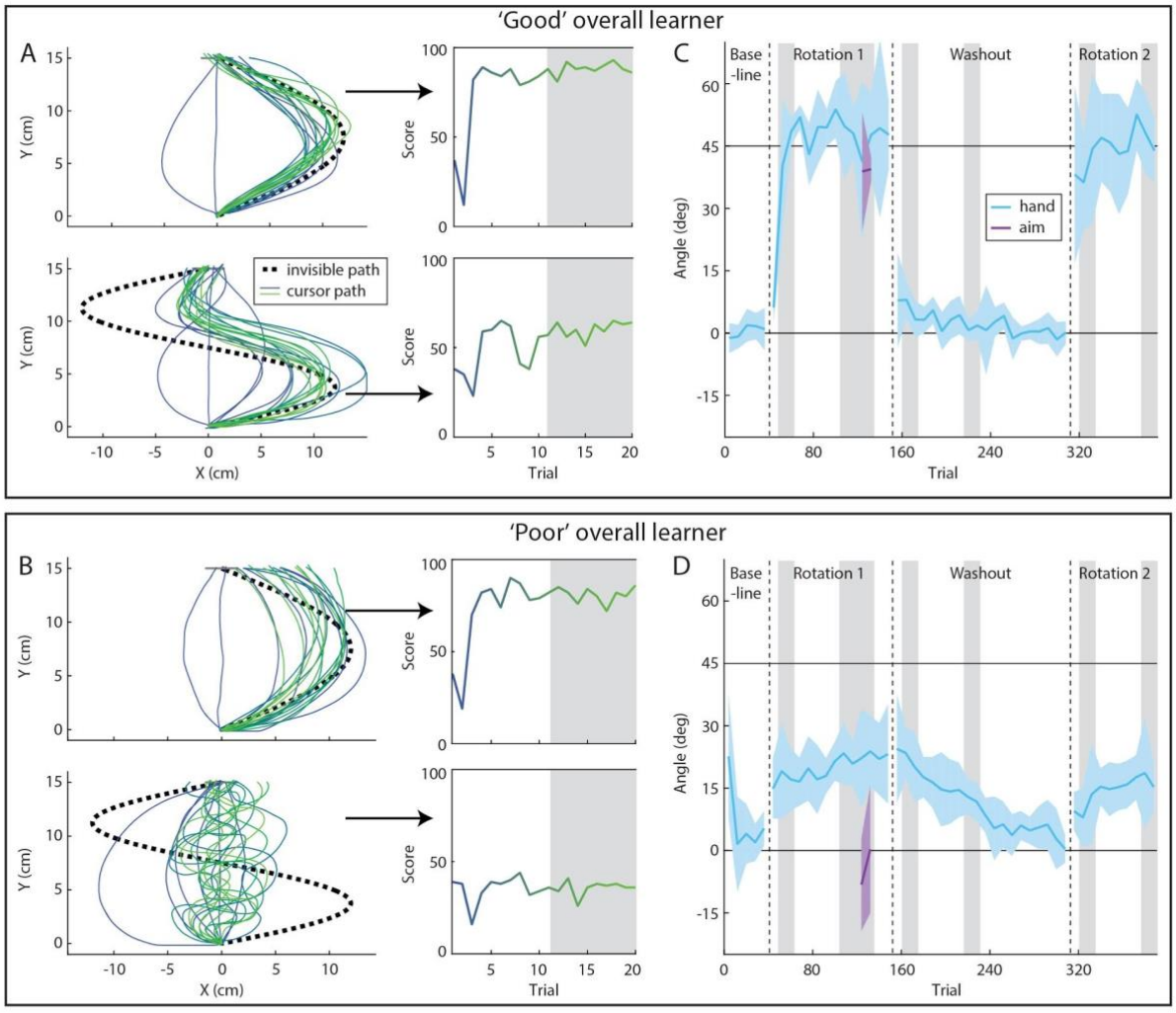

222

Figure 2. Learning performance in the error-based and reward-based tasks is related and is captured by a single latent variable. (A,C) Data of an example 'good learner'. (A) shows the hidden path (dashed black line), drawn paths (blue and green lines), and score (blue to green gradient) for two blocks in the reward-based learning task. The median score in the last 10 trials of each block (grey shaded area) was used in further analyses. (C) shows the hand angle (light blue) and reported aiming angle (purple) relative to the target angle during the error-based learning task. Each data point represents the median of a set of eight trials, and the shading represents ± one standard deviation. The mean scores across sets 2 and 3 (early learning) and 9 and 10 (late learning) of the rotation and washout blocks were used in further analyses, as well as the averaged aiming angle (grey shaded areas). In the baseline and washout blocks, a hand angle of zero would result in a target hit, and in the rotation blocks, a hand angle of 45° results in perfect compensation of the rotated cursor path, and thus a target hit. (B,D) Same as (A,C), but for a 'poor learner'. (E) Correlations between scores in the reward-based and error-based motor learning task across participants (n=33). (F) Principal component analysis loadings for the first and second principal component.

Larger entorhinal volume is associated with better motor learning

Having clearly established that performance in reward-based and error-based learning is related, our next aim was to determine whether such performance is associated with the neuroanatomy of the MTL. To this end, we performed multiple linear regression analyses to predict PC1 and PC2 based on the right and left hippocampus (HC) and entorhinal cortex (EC) volumes (Fig. 3AB), corrected for total intracranial volume (see *Methods*). We also included total intracranial (IC) volume in our model to account for a potential effect of overall head size. Figure 3C shows the standardized regression coefficients and 95% confidence interval of the regression models for each PC. For PC1— our measure of performance in both tasks—the model explained 36.0% of the variance in PC1 score (model $F(5)=3.030$, $p=0.027$; Table S1), with right EC volume being the only significant predictor of PC1 score ($t=3.318$, $p=0.003$). That is, greater right entorhinal volume corresponded with higher scores on PC1, or better learning in both tasks. Notably, we found no significant predictors of PC2 score (model $F(5)=0.454$, $p=0.806$, $R_2=7.8\%$). This lack of effect might not be surprising given that the percentage of variance in our motor learning data that was explained by the second principal component was quite small (13.4%).

As a secondary analysis, we performed a linear regression with the anterior and posterior hippocampus as separate predictors, as previous studies have reported differential relationships between these individual parts of the hippocampus and memory (e.g., 50). However, here we again did not find significant relationships between left and right aHC and pHC volume and the score on PC1 (model $F(5)=0.358$, $p=0.427$, $R_2=6.2\%$) or PC2 ($F(5)=0.939$, $p=0.472$, $R_2=14.8\%$;

Table S2). See the *Supplemental Results* for exploratory regression analyses using participants' striatal volumes as predictors.

Taken together, the results of these regression analyses indicate that better performance in both reward-based and error-based learning is associated with larger right entorhinal volume.

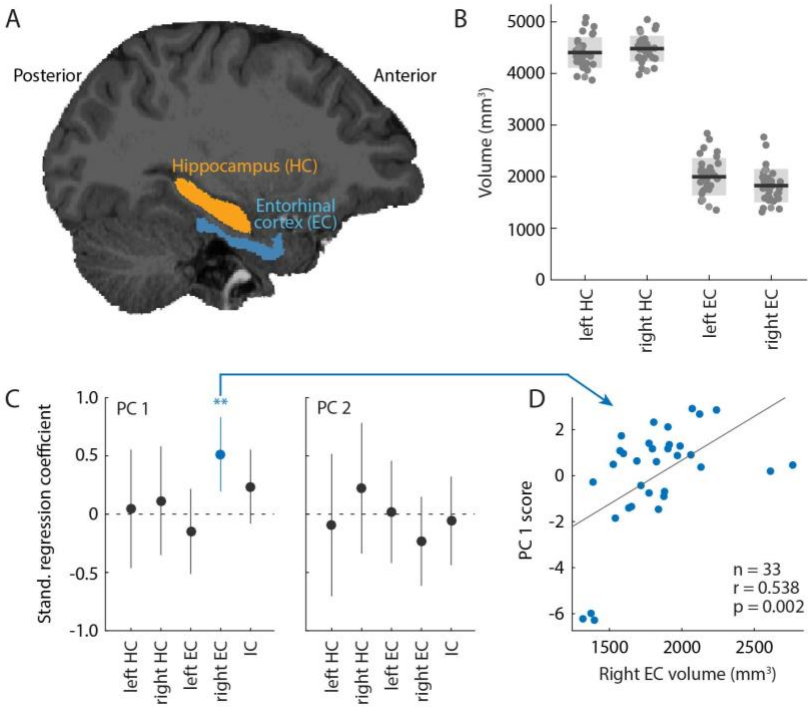

Figure 3. Larger entorhinal volumes are uniquely associated with better overall motor learning. (A) Illustration of the segmented hippocampus (orange) and entorhinal cortex (blue) in an example participant. (B) Volume of the left (L) and right (R) hippocampus (HC) and entorhinal cortex (EC), corrected for total intracranial volume (see *Methods*). Each dot depicts an individual participant (n=33), the dark grey line indicates the mean across participants, and the light grey area indicates the standard deviation. (C) Standardized regression coefficients and their corresponding 95% confidence intervals of the regression models to predict principal component 1 (PC 1; left panel) and principal component 2 (PC 2; right panel) based on the left and right hippocampus and entorhinal volumes, and the total intracranial volume (IC). (D) Individual partial correlation between right entorhinal volume and PC 1 score. The line represents the best fit regression line.

Discussion

While previous work in motor learning has often studied error-based and reward-based learning processes in isolation from one another, recently there has been increased interest in

understanding how these separate learning processes interact at the behavioral and neural levels. Here we find a strong relationship in intersubject variability between error-based and reward-based motor learning, showing that learning performance across tasks can be explained by a single, latent variable. Our measures of learning and the nature of the tasks used suggest that this latent variable captures participants' use of cognitive strategies during learning, with higher scores on this variable being associated with faster and better overall learning in both tasks. We further show, using structural neuroimaging and regression analyses with participants' hippocampus and entorhinal cortical volumes as predictors, that higher scores on this latent variable, and thus faster and better overall learning, are associated with larger right entorhinal volume. Together, these findings suggest that a shared strategic process underlies individual differences in error-based and reward-based motor learning, and that this process is associated with structural differences in entorhinal cortex.

Considerable computational and neural work has argued for a division of labor between the neural circuits that support error-based and reward-based learning (8, 31, 34, 59–61). According to this prevailing view, cortico-cerebellar pathways are responsible for error-based learning whereas cortico-striatal pathways are responsible for reward-based learning. Such distinctions, however, have often been reliant on indirect comparisons between different studies, and have been influenced by sampling biases in neural recording sites across different tasks. For instance, conventional views on error-based learning have suggested that adaptation is a primarily automatic mechanism, immune to reward-based feedback (8, 34). However, more recent behavioral evidence suggests that these two learning processes, while separable (62, 63), interact during sensorimotor learning (7, 64–66). Such interactions are likely to be supported by the recent demonstration of direct anatomical connections between the cerebellum and striatum (67). These bidirectional connections could explain recent neural findings from rodents showing that the cerebellum, besides processing direction-related errors, also represents various aspects of reward-related information during task performance (68–71). Together, this emerging evidence suggests that error-based and reward-based learning processes are closely intertwined at both the behavioral and neural levels.

There is also emerging evidence to suggest that both error-based and reward-based processes are mediated through the use of cognitive strategies implemented during learning. In error-based adaptation, the contribution of this explicit, declarative process to learning has been well-established behaviorally (2, 3, 13, 19, 23, 24, 72). Recent evidence from our group further

311 indicates that faster learning across participants is linked to individual differences in the magnitude
312 of the cognitive strategy (3), which drives rapid changes early in the learning process. In reward-
313 based learning, by contrast, the contribution of cognitive strategies have received comparably
314 little attention, and is only beginning to be established. As one example, recent work (36) using a
315 visuomotor rotation task, wherein participants were only provided with reward-based feedback
316 (binary success/failure), has shown that good versus poor learning is related to the
317 implementation of a large cognitive component. This was evidenced by the observed reduction in
318 reach angle when participants were required to remove their aiming strategy (see also 35). It was
319 also evidenced by the observation that the reward-based learning was impaired when (1)
320 participants had to perform a dual task (a separate mental rotation task) that divided their cognitive
321 load (36), or when (2) participants' reaction times were constrained (35), such that they could not
322 implement the strategy (72). To date, work examining the link between error- and reward-based
323 (63, 64, 66), has focused on how reinforcement signals (e.g., binary success/failure) shape both
324 forms of learning. By contrast, our current behavioral findings show that, even when distinct
325 reward- and error-based learning tasks are used, there is a single latent variable that explains a
326 significant proportion of intersubject variability in performance across both types of learning.
327
328 We found that a larger right entorhinal volume was associated with better overall learning in both
329 the reward-based and error-based motor learning tasks. The entorhinal cortex has been shown
330 to support a wide range of cognitive functions that would have bearing on various features of our
331 motor learning tasks. Classically, the entorhinal cortex, together with neighboring areas in the
332 medial temporal lobe, has been implicated in spatial navigation and memory through
333 electrophysiological studies in rodents. These studies showed that place cells in the hippocampus
334 (73) and grid cells in the entorhinal cortex (74) form a map-like representation of the environment.
335 Grid cells have also been demonstrated in primate entorhinal cortex, even in the absence of
336 locomotion, when the animal is simply exploring a visual scene with its eyes (75, 76). Such
337 observations have recently been extended to humans with functional MRI (77, 78), and there is
338 even evidence suggesting that mere shifts in covert attention (i.e., in the absence of overt eye
339 movements), also elicits grid-cell-like responses in the entorhinal cortex (79). Together, these and
340 other findings (51, 52, 80) have begun to reshape our understanding of the role of the entorhinal
341 cortex in visual-spatial memory, and more generally in cognitive operations. An influential
342 hypothesis is that the hippocampal-entorhinal system supports a cognitive map, an idea that was
343 originally proposed to explain findings in rodents (55, 56) and later extended to humans (for review

see 81). This hypothesis proposes that the brain creates flexible representations of the environment to not only support memory but also guide effective (motor) behavior (42, 82, 83).

In the context of the current study, we expect cognitive and spatial maps to be utilized during the exploration of visuomotor space in our curve drawing and visuomotor rotation tasks. Studies using fMRI in healthy adults, and neural recordings or electrical stimulation in pre-surgical patients, have provided evidence that the entorhinal cortex supports the encoding of goal direction and distance, relative locations, and the clockwise or counterclockwise direction of routes (84–90). While our motor learning tasks did not involve navigation in VR, the encoding of goal directions (in the visuomotor rotation task) and trajectories to the goal (in the curve drawing task) were critical to learning. If the entorhinal cortex is important for representing such spatial information, then its size may predict the ability to perform tasks — perceptual and motor — that recruit such representations. Studies investigating the relation between neuroanatomy and performance have associated greater gray matter volume in the entorhinal cortex with better scene recognition (46), spatial memory (45), navigation to memorized object locations in VR (47), as well as the lifetime amount of video gaming (91). Here, we extend these general observations to include the domain of motor learning, showing an association between entorhinal volume and overall performance in error-based and reward-based learning tasks. Although the basis for our lateralized right hemispheric effects are unclear, we find it noteworthy that it is primarily the right, and not left, regions of the medial temporal lobe that are associated with the processing of spatial information (92).

Methods

This study was part of a larger cohort study (registered at https://osf.io/y8649) in which 66 right-handed paid volunteers underwent structural and resting state MRI scans. We anticipated that a subgroup of ~40 participants would agree to perform the error-based and reward-based motor learning tasks following participation in this main study. Thirty-four participants (18 men and 16 women, aged 20-35 years) actually took part in these separate sessions (51 days before to 98 days after the MRI session, mean absolute difference 38 days). One of these participants was excluded from further analysis because of a high number of invalid trials in the error-based learning task (>25%), thus leaving 33 participants for analysis.

The main experiment and motor learning follow-up tasks were approved by the Queen's University Health Sciences Research Ethics Board, and participants provided written informed consent before participating in the MRI session and in the motor learning sessions. The methods and data analyses for the current study are pre-registered on OSF (https://osf.io/7prq5).

Neuroimaging

Procedure

The day prior to each participants' MRI scan, participants completed a biofeedback session in a simulated (mock) MRI scanner to become familiar with the MRI environment and to learn to minimize head movement. During the biofeedback session, participants viewed a 45-minute documentary with a live readout trace of their head motion overlaid. When their head motion exceeded an adaptive threshold, the documentary was paused for several seconds while static was played on the screen along with a loud, unpleasant noise. The next day, MRI data were collected over the course of a 1.5-hour session using a 3T whole-body MRI scanner (Magnetom Tim Trio; Siemens Healthcare). We gathered high-resolution whole-brain T1-weighted (repetition time [TR] 2400 ms; echo time [TE] 2.13 ms; flip angle 8°; echo spacing 6.5 ms) and T2-weighted (TR 3200 ms; TE 567 ms; variable flip angle; echo spacing 3.74 ms) anatomical images (in-plane resolution 0.7 × 0.7 mm_2; 320 × 320 matrix; slice thickness 0.7 mm; 256 AC-PC transverse slices; anterior-to-posterior encoding; 2 × acceleration factor) and an ultra-high resolution T2-weighted volume centred on the medial temporal lobes (resolution 0.5 x 0.5 mm_2; 384 × 384 matrix; slice thickness 0.5 mm; 104 transverse slices acquired parallel to the hippocampus long axis; anterior-to-posterior encoding; 2 x acceleration factor; TR 3200 ms; TE 351 ms; variable flip angle; echo spacing 5.12 ms). The whole brain protocols were selected on the basis of protocol optimizations designed by Sortiropoulos and colleagues (93). The hippocampal protocols were modeled after Chadwick and colleagues (94). In addition, we acquired two sets (right-left direction and left-right direction) of whole-brain diffusion-weighted volumes (64 directions, b = 1200 s/mm_2, 93 slices, voxel size = 1.5 × 1.5 × 1.5 mm_3, TR 5.18 s, TE 103.4 ms; 3 times multiband acceleration), plus two extra B0 scans gathered separately for each orientation.

Data analysis

Automated cortical and subcortical segmentation of the T1-weighted and T2-weighted brain data was performed in Freesurfer (v6.0) (95, 96). For each hemisphere, we obtained the volume of the hippocampus (HC) and entorhinal cortex (EC) in the MTL for our main analysis. We also obtained

406 striatal volumes, including left and right globus pallidus, putamen, caudate and accumbens for
407 exploratory analyses (see *Supplemental Information*). Segmentations of these areas were
408 checked visually and manually adjusted if necessary.
409
410 In addition to the Freesurfer segmentations, we obtained separate volumetric measures of the
411 anterior and posterior hippocampus in each hemisphere. The ultra-high-resolution T2-weighted
412 0.5mm isotropic medial temporal lobe scans were submitted to automated segmentation using
413 HIPS, an algorithm previously validated to human raters specialized in segmenting detailed
414 neuroanatomical scans of the hippocampus (97). Three independent raters were trained on
415 segmenting the hippocampus at the uncal apex into aHC and pHC segments, and achieved a
416 Dice coefficient of absolute agreement of 80%. Two of these raters independently segmented all
417 participants using the 0.5 mm T1-weighted scans. The T2-weighted medial temporal lobe scans
418 were registered to the T2-weighted whole-brain scans, which were in turn registered to the T1-
419 weighted whole-brain scans, and the combined transform was used to place the rater landmarks
420 on the detailed medial temporal lobe scans. Finally, the total number of voxels in each subregion
421 was multiplied by the volume of each voxel to obtain a total aHC and pHC volume.
422
423 To account for differences in head size, all regional volumes were corrected for total intracranial
424 (IC) volume obtained from Freesurfer. This was done by first estimating the slope b of the
425 regression line of each regional volume on the IC volume across the 33 participants included in
426 the analysis. Next, each regional volume was adjusted for the IC volume as: adjusted volume =
427 raw volume - b × (IC volume - mean IC volume).

428 ## *Motor Learning Tasks*

429 ### Procedure

430 Thirty-four participants performed an error-based and a reward-based motor learning task. We
431 attempted to fully counterbalance the tasks across participants; The first 19 participants
432 performed the error-based motor learning task before performing the reward-based motor
433 learning task, with the next 15 participants performing the reward-based motor learning task
434 before the error-based motor learning task. The reward-based task took about 25 minutes to
435 complete and the error-based task took about 65 minutes to complete.

Setup

Participants were seated at a table, with their chin and forehead supported by a headrest placed ~50 cm in front of a vertical LCD monitor (display size 47.5 × 26.5 cm; resolution 1920 × 1080 pixels) on which the stimuli were presented (Fig. 1A). Participants performed reaching movements by sliding a stylus across a digital drawing tablet (active area 311 x 216 mm; Wacom Intuous) placed on the table in front of the participant. Movement trajectories were sampled at 100 Hz by the digitizing tablet. Vision of the hand and tablet was occluded by a piece of black cardboard attached to the headrest. In the error-based learning task, eye movements were tracked at 500 Hz using a video-based eye tracker (Eyelink 1000; SR Research) placed beneath the monitor. The eye movement data were not analyzed in this study. The stimuli and motor learning tasks are described in detail below.

Reward-based motor learning

Task

The task was inspired by the reward-based learning task designed by Dam and colleagues (57). Participants performed reaching movements from a start position to a target line by sliding the stylus across the tablet. They were instructed to “find an invisible curved path by drawing paths on the tablet and evaluating your score for each attempt”. Participants started with a practice block of 10 trials, in which they traced a visible, straight line between the start position and the target, to become familiar with the task and the timing requirement of performing the movement within 2 s. Next, participants performed 12 blocks, each containing 20 attempts to copy an invisible path, which differed in each block.

Each trial started with the presentation of a start position (5 mm radius circle). After the participant had moved the cursor to the start position and held it there for 200 ms, a horizontal target line (30 x 1 mm) would appear 15 cm in front of the start position, and a rectangular outlined box (320 x 170 mm) would appear around the start position and target (Fig. 1B). Next, participants drew a path from the start position to the target line while remaining in the box. After crossing the target line, the cursor disappeared, and a score between 0 and 100 was displayed centrally (for 1 s), indicating how close they were to the invisible path. Following this, all stimuli disappeared, and a new trial would start with the presentation of the start position and the reappearance of the cursor. If the movement duration was longer than 2 s, the score was not presented and the trial was repeated.

The invisible paths consisted of single curves (i.e., half sine waves; 6 blocks) and double curves (i.e., full sine waves; 6 blocks) of different amplitudes (± 0.2, 0.5 and 0.8 times the target distance), drawn between the start position and the center of the target line. Participants were not informed about the possible shapes of the invisible lines. The trial score was computed by taking the x position of the cursor at every cm travelled in the y-direction (i.e., 1, 2, 3, … and 15 cm), and computing the absolute difference in x position between the cursor and the invisible line at the corresponding y-distance. The sum of these errors was then normalized by dividing it by the sum of distances between a straight line and a curve with an amplitude of 0.5 times the target distance, and multiplied by 100 to obtain a score between 0 and 100 (negative scores were presented as 0).

All participants performed one practice block and 12 experimental blocks of trials. Ten different randomized orders of experimental blocks were created. Participant 1, 11, 21, and 31 performed the first order, participant 2, 12, 22, and 32 performed the second order, etc.

Data analysis

The median score in trials 11 to 20 of each block of 20 attempts were used as a measure of learning performance. We did not use trials 1-10 in our analysis based on our observation that, for participants who learned fairly quickly, they often used exploratory strategies when encountering a new path, which frequently resulted in scores of, or around, zero (Fig. 2A provides a good example of such a participant). For each participant, we averaged the median scores across single curves with the same amplitude (i.e. ‘leftward’ and ‘rightward’ curves) and across double curves with the same amplitude. This resulted in six scores per participant.

Error-based motor learning

Task

Participants performed center-out reaching movements from a start position to one of eight visual targets presented on a 10 cm radius ring around the start position. Participants were instructed to hit the target with their cursor by making a fast reaching movement on the tablet, ‘slicing’ through the target. The ratio between movement of the tip of the stylus and movement of the cursor presented on the screen was 1:2, so that a movement of 5 cm on the tablet corresponded to a movement of 10 cm of the cursor. Participants first performed a baseline block in which they

499 received veridical feedback about the position of the tip of the stylus, shown as a cursor on the
500 screen. After performing a baseline block, participants performed a visuomotor rotation task, a
501 task that has been used extensively to assess error-based learning (e.g., 58, 98). In this task, the
502 movement of the cursor representing the hand position is rotated about the hand start location, in
503 this experiment by 45º clockwise, requiring that a counterclockwise adjustment of movement
504 direction be learned.
505
506 Each trial started with the participant moving the stylus to a central start position (5 mm radius
507 circle). When the (unseen) cursor was within 5 cm of the start position, a ring was presented
508 around the start position to indicate the distance of the cursor, so that the participant had to reduce
509 the size of the ring to move to the start position. The cursor (4 mm radius circle) appeared when
510 the cursor 'touched' the start position (9 mm distance). After the cursor was held within the start
511 position for 500 ms, the target (6 mm radius open circle) was presented on an (imaginary) 10 cm
512 radius ring around the start position at one of eight locations, separated by 45º (i.e., 0, 45, 90,
513 135, 180, 225, 270 and 315º). In addition, 64 non-target 'landmarks' (3 mm radius outlined circles,
514 spaced 5.625º apart) were presented, forming a 10 cm radius ring around the start position. After
515 a 2 s delay, the target would 'fill in' (i.e., color red), providing the cue for the participant to perform
516 a fast movement to the target. If the participant started the movement before the cue, or more
517 than 1 s after the cue, the trial was aborted and a feedback message indicating "Too early" or
518 "Too late" appeared on the screen, respectively. In correctly timed trials, the cursor was visible
519 during the movement to the ring and then became stationary for 1 s when it reached the ring,
520 providing the participant with visual feedback of their endpoint error. When any part of the cursor
521 overlapped with any part of the target, the target would color green to indicate a hit. If the duration
522 of the movement was longer than 300 ms, a feedback message "Too slow" would appear on the
523 screen.
524
525 In trials in the rotation block, the movement of the cursor was rotated by 45º clockwise around the
526 start position. To assess the contribution of the explicit process of learning, participants performed
527 several 'reporting' trials. These trials were performed at the end of the first rotation block to ensure
528 that participants' learning behavior would not be influenced, as the reporting procedure itself can
529 increase the proportion of participants that implement a cognitive strategy (3). In reporting trials,
530 participants were instructed to, before each reach movement, report the aiming direction of their
531 hand for the cursor to hit the target. They did this by turning a knob with their left hand, to rotate
532 a line on the screen, positioned between the start position and the ring, to align it with their

strategic aimpoint. When satisfied with the direction of the line, the participant clicked a button positioned next to the knob, and the line disappeared. After a 1 s delay, the target filled in as a cue to execute the reach.

All participants performed 4 blocks of trials in total, where within each block, target locations were randomized within sets of eight: (1) A baseline block (5 sets of 8 trials; 40 in total), (2) a rotation block (10 sets of 8 trials without report + 2 sets of 8 reporting trials + 2 sets of 8 trials without report; 112 trials in total), (3) a washout block in which veridical cursor feedback was restored (10 + 10 sets with a 30 s break in between; 160 trials in total) and (4) a second rotation block to assess participants' rates of re-learning (10 sets of 8 trials; 80 in total). Ten different randomized trial orders were created for the full experiment. Participant 1, 11, 21, and 31 performed the first order, participant 2, 12, 22, and 32 performed the second order, etc.

Data analysis

Trials in which the movement was initiated too early or too late (as detected online; 4% of trials) or in which the movement duration was longer than 300 ms (4% of trials), were discarded from the analysis. The median endpoint hand angle (i.e., the difference in angle between the target and the hand when the cursor crossed the ring) per set of eight trials was used as a measure of learning performance. For each participant, we computed early and late learning scores in the first rotation block, washout block, and second rotation block. To do this, we averaged the median in sets 2 and 3 and in sets 9 and 10 of each of these blocks (excluding the first set in which participants often showed highly variable behavior). To derive a measure of the magnitude of the explicit component of learning, we used the average of the median reported aiming angle with respect to the target, obtained in the reporting trials (sets 11 and 12 in the rotation block). This resulted in seven measures per participant.

Relating learning measures and neuroanatomy

Since the learning scores within and between the two learning tasks showed significant correlations across participants, we first submitted the scores to a principal component analysis (PCA) to obtain measures of learning performance across single dimensions. To do this, we first transformed the variables. For the error-based learning task, all angles were converted to absolute errors with respect to the target, and then multiplied by -1 so that positive values correspond to better performance. We then standardized all scores before submitting them to the PCA. The principal components (PCs) were obtained using the pca function in Matlab, which uses

a singular value decomposition algorithm. PCA reduces the dimensionality of the data by finding PCs that capture the maximal variance in the data.

To test the hypothesis that better performance in the motor learning tasks is related to greater volumes of brain areas in the medial temporal lobe, we performed multiple linear regression analyses. All models were estimated using the fitlm function in Matlab, which returns a least-squares fit of the scores to the data. Our primary analysis included the left and right HC and EC volumes. To control for a potential effect of overall head size on learning performance, we also included each participant's total intracranial volume, making a total of five neuroanatomical measures. For the first and second PC, we fitted a multiple linear regression model with the PC as the dependent variable, and the set of four regional volumes plus the IC volume as predictors. Previous studies have reported differential relationships between the anterior and posterior parts of the hippocampus and memory (e.g., 50). Therefore, we performed a secondary analysis, including the left and right anterior and posterior HC volume as predictors, and the IC volume as a confounder.

Author contributions

Conceptualization and methodology AJdB, JP, JPG, JRF; investigation AJdB; software AJdB; formal analysis AJdB, JP, MRR; visualization AJdB, JPG, MRR; writing - original draft AJdB, JPG; writing - review and editing AJdB, JP, JPG, JRF, MRR; supervision AJdB, JP, JPG; project administration AJdB, JP, JPG; resources JP, JPG, JRF; funding acquisition JP, JPG, JRF.

Acknowledgements

The authors thank Mohammed Albaghdadi, Olivia Broda, Sydney Dore, Kate McKenzie and Reem Toubache for help with data collection, and Martin York for technical support.

References

1. H. G. Wu, Y. R. Miyamoto, L. N. Gonzalez Castro, B. P. Ölveczky, M. A. Smith, Temporal structure of motor variability is dynamically regulated and predicts motor learning ability. *Nat. Neurosci.* **17**, 312–321 (2014).

2. J. Fernandez-Ruiz, W. Wong, I. T. Armstrong, J. R. Flanagan, Relation between reaction time and reach errors during visuomotor adaptation. *Behav. Brain Res.* **219**, 8–14 (2011).

3. A. J. de Brouwer, M. Albaghdadi, J. R. Flanagan, J. P. Gallivan, Using gaze behavior to parcellate the explicit and implicit contributions to visuomotor learning. *J. Neurophysiol.* **120**, 1602–1615 (2018).

4. A. Stark-Inbar, M. Raza, J. A. Taylor, R. B. Ivry, Individual differences in implicit motor learning: task specificity in sensorimotor adaptation and sequence learning. *J. Neurophysiol.* **117**, 412–428 (2017).

5. K. M. Trewartha, A. Garcia, D. M. Wolpert, J. R. Flanagan, Fast but fleeting: adaptive motor learning processes associated with aging and cognitive decline. *J. Neurosci.* **34**, 13411–13421 (2014).

6. J. A. Anguera, P. A. Reuter-Lorenz, D. T. Willingham, R. D. Seidler, Contributions of spatial working memory to visuomotor learning. *J. Cogn. Neurosci.* **22**, 1917–1930 (2010).

7. J. A. Taylor, R. B. Ivry, Cerebellar and prefrontal cortex contributions to adaptation, strategies, and reinforcement learning. *Prog. Brain Res.* **210**, 217–253 (2014).

8. K. Doya, Complementary roles of basal ganglia and cerebellum in learning and motor control. *Curr. Opin. Neurobiol.* **10**, 732–739 (2000).

9. H. Lalazar, E. Vaadia, Neural basis of sensorimotor learning: modifying internal models. *Curr. Opin. Neurobiol.* **18**, 573–581 (2008).

10. R. D. Seidler, J. Bo, J. A. Anguera, Neurocognitive contributions to motor skill learning: the role of working memory. *J. Mot. Behav.* **44**, 445–453 (2012).

11. S. Corkin, Acquisition of motor skill after bilateral medial temporal-lobe excision. *Neuropsychologia* **6**, 255–265 (1968).

12. B. Milner, “Memory disturbance after bilateral hippocampal lesions” in *Cognitive Processes and the Brain*, P. M. Milner, S. E. Glickman, Eds. (Van Nostrand, 1965), pp. 97–111.

13. J. A. Taylor, R. B. Ivry, Flexible cognitive strategies during motor learning. *PLoS Comput. Biol.* **7**, e1001096 (2011).

14. P. Mazzoni, J. W. Krakauer, An implicit plan overrides an explicit strategy during visuomotor adaptation. *J. Neurosci.* **26**, 3642–3645 (2006).

15. A. Keisler, R. Shadmehr, A shared resource between declarative memory and motor memory. *J. Neurosci.* **30**, 14817–14823 (2010).

16. S. Werner, O. Bock, Effects of variable practice and declarative knowledge on sensorimotor adaptation to rotated visual feedback. *Exp. Brain Res.* **178**, 554–559 (2007).

17. R. Shadmehr, M. A. Smith, J. W. Krakauer, Error correction, sensory prediction, and adaptation in motor control. *Annu. Rev. Neurosci.* **33**, 89–108 (2010).

18. D. M. Wolpert, J. Diedrichsen, J. R. Flanagan, Principles of sensorimotor learning. *Nat. Rev. Neurosci.* **12**, 739–751 (2011).

19. J. A. Taylor, J. W. Krakauer, R. B. Ivry, Explicit and implicit contributions to learning in a sensorimotor adaptation task. *J. Neurosci.* **34**, 3023–3032 (2014).

20. S. M. Morton, A. J. Bastian, Cerebellar contributions to locomotor adaptations during splitbelt treadmill walking. *J. Neurosci.* **26**, 9107–9116 (2006).

21. M. A. Smith, R. Shadmehr, Intact ability to learn internal models of arm dynamics in Huntington's disease but not cerebellar degeneration. *J. Neurophysiol.* **93**, 2809–2821 (2005).

22. Y.-W. Tseng, J. Diedrichsen, J. W. Krakauer, R. Shadmehr, A. J. Bastian, Sensory prediction errors drive cerebellum-dependent adaptation of reaching. *J. Neurophysiol.* **98**, 54–62 (2007).

23. G. M. Redding, B. Wallace, Adaptive coordination and alignment of eye and hand. *J. Mot. Behav.* **25**, 75–88 (1993).

24. K. M. Bond, J. A. Taylor, Flexible explicit but rigid implicit learning in a visuomotor adaptation task. *Journal of Neurophysiology* **113**, 3836–3849 (2015).

25. J. R. Morehead, J. A. Taylor, D. E. Parvin, R. B. Ivry, Characteristics of Implicit Sensorimotor Adaptation Revealed by Task-irrelevant Clamped Feedback. *J. Cogn. Neurosci.* **29**, 1061–1074 (2017).

26. V. Della-Maggiore, A. R. McIntosh, Time course of changes in brain activity and functional connectivity associated with long-term adaptation to a rotational transformation. *J. Neurophysiol.* **93**, 2254–2262 (2005).

27. A. Floyer-Lea, P. M. Matthews, Changing brain networks for visuomotor control with increased movement automaticity. *J. Neurophysiol.* **92**, 2405–2412 (2004).

28. R. Shadmehr, H. H. Holcomb, Neural correlates of motor memory consolidation. *Science* **277**, 821–825 (1997).

29. J. Doyon, H. Benali, Reorganization and plasticity in the adult brain during learning of motor skills. *Curr. Opin. Neurobiol.* **15**, 161–167 (2005).

30. P. Dayan, Y. Niv, Reinforcement learning: the good, the bad and the ugly. *Curr. Opin. Neurobiol.* **18**, 185–196 (2008).

31. M. Ito, K. Doya, Multiple representations and algorithms for reinforcement learning in the cortico-basal ganglia circuit. *Curr. Opin. Neurobiol.* **21**, 368–373 (2011).

32. R. S. Sutton, A. G. Barto, *Reinforcement Learning: An Introduction* (A Bradford Book,

2018).

33. J. R. Wickens, J. N. J. Reynolds, B. I. Hyland, Neural mechanisms of reward-related motor learning. *Curr. Opin. Neurobiol.* **13**, 685–690 (2003).

34. R. Shadmehr, J. W. Krakauer, A computational neuroanatomy for motor control. *Exp. Brain Res.* **185**, 359–381 (2008).

35. O. Codol, P. J. Holland, J. M. Galea, The relationship between reinforcement and explicit control during visuomotor adaptation. *Sci. Rep.* **8**, 9121 (2018).

36. P. Holland, O. Codol, J. M. Galea, Contribution of explicit processes to reinforcement-based motor learning. *J. Neurophysiol.* **119**, 2241–2255 (2018).

37. K. Duncan, B. B. Doll, N. D. Daw, D. Shohamy, More Than the Sum of Its Parts: A Role for the Hippocampus in Configural Reinforcement Learning. *Neuron* **98**, 645–657.e6 (2018).

38. S. J. Gershman, N. D. Daw, Reinforcement Learning and Episodic Memory in Humans and Animals: An Integrative Framework. *Annu. Rev. Psychol.* **68**, 101–128 (2017).

39. N. Burgess, E. A. Maguire, J. O'Keefe, The Human Hippocampus and Spatial and Episodic Memory. *Neuron* **35**, 625–641 (2002).

40. L. R. Squire, S. Zola-Morgan, The medial temporal lobe memory system. *Science* **253**, 1380–1386 (1991).

41. H. Eichenbaum, N. J. Cohen, Can we reconcile the declarative memory and spatial navigation views on hippocampal function? *Neuron* **83**, 764–770 (2014).

42. J. L. S. Bellmund, P. Gärdenfors, E. I. Moser, C. F. Doeller, Navigating cognition: Spatial codes for human thinking. *Science* **362** (2018).

43. K. M. Rodrigue, N. Raz, Shrinkage of the entorhinal cortex over five years predicts memory performance in healthy adults. *J. Neurosci.* **24**, 956–963 (2004).

44. A. P. Yonelinas, *et al.*, Memory in the aging brain: doubly dissociating the contribution of the hippocampus and entorhinal cortex. *Hippocampus* **17**, 1134–1140 (2007).

45. T. Hartley, R. Harlow, An association between human hippocampal volume and topographical memory in healthy young adults. *Front. Hum. Neurosci.* **6**, 338 (2012).

46. A. S. Whiteman, D. E. Young, A. E. Budson, C. E. Stern, K. Schon, Entorhinal volume, aerobic fitness, and recognition memory in healthy young adults: A voxel-based morphometry study. *Neuroimage* **126**, 229–238 (2016).

47. K. R. Sherrill, E. R. Chrastil, I. Aselcioglu, M. E. Hasselmo, C. E. Stern, Structural Differences in Hippocampal and Entorhinal Gray Matter Volume Support Individual Differences in First Person Navigational Ability. *Neuroscience* **380**, 123–131 (2018).

48. V. R. Schinazi, D. Nardi, N. S. Newcombe, T. F. Shipley, R. A. Epstein, Hippocampal size predicts rapid learning of a cognitive map in humans. *Hippocampus* **23**, 515–528 (2013).

49. T. I. Brown, A. S. Whiteman, I. Aselcioglu, C. E. Stern, Structural differences in

hippocampal and prefrontal gray matter volume support flexible context-dependent navigation ability. *J. Neurosci.* **34**, 2314–2320 (2014).

50. E. A. Maguire, *et al.*, Navigation-related structural change in the hippocampi of taxi drivers. *Proc. Natl. Acad. Sci. U. S. A.* **97**, 4398–4403 (2000).

51. A. J. Horner, J. A. Bisby, E. Zotow, D. Bush, N. Burgess, Grid-like Processing of Imagined Navigation. *Curr. Biol.* **26**, 842–847 (2016).

52. A. O. Constantinescu, J. X. O'Reilly, T. E. J. Behrens, Organizing conceptual knowledge in humans with a gridlike code. *Science* **352**, 1464–1468 (2016).

53. D. Aronov, R. Nevers, D. W. Tank, Mapping of a non-spatial dimension by the hippocampal-entorhinal circuit. *Nature* **543**, 719–722 (2017).

54. R. M. Tavares, *et al.*, A Map for Social Navigation in the Human Brain. *Neuron* **87**, 231–243 (2015).

55. E. C. Tolman, Cognitive maps in rats and men. *Psychol. Rev.* **55**, 189–208 (1948).

56. J. O'Keefe, L. Nadel, *The hippocampus as a cognitive map* (Oxford University Press, USA, 1978).

57. G. Dam, K. Kording, K. Wei, Credit assignment during movement reinforcement learning. *PLoS One* **8**, e55352 (2013).

58. H. A. Cunningham, Aiming error under transformed spatial mappings suggests a structure for visual-motor maps. *J. Exp. Psychol. Hum. Percept. Perform.* **15**, 493–506 (1989).

59. K. Doya, What are the computations of the cerebellum, the basal ganglia and the cerebral cortex? *Neural Netw.* **12**, 961–974 (1999).

60. N. D. Daw, K. Doya, The computational neurobiology of learning and reward. *Curr. Opin. Neurobiol.* **16**, 199–204 (2006).

61. H. Makino, E. J. Hwang, N. G. Hedrick, T. Komiyama, Circuit Mechanisms of Sensorimotor Learning. *Neuron* **92**, 705–721 (2016).

62. J. Izawa, R. Shadmehr, Learning from sensory and reward prediction errors during motor adaptation. *PLoS Comput. Biol.* **7**, e1002012 (2011).

63. J. G. A. Cashaback, H. R. McGregor, A. Mohatarem, P. L. Gribble, Dissociating error-based and reinforcement-based loss functions during sensorimotor learning. *PLoS Comput. Biol.* **13**, e1005623 (2017).

64. L. Shmuelof, *et al.*, Overcoming motor "forgetting" through reinforcement of learned actions. *J. Neurosci.* **32**, 14617–14621 (2012).

65. A. A. Nikooyan, A. A. Ahmed, Reward feedback accelerates motor learning. *J. Neurophysiol.* **113**, 633–646 (2015).

66. J. M. Galea, E. Mallia, J. Rothwell, J. Diedrichsen, The dissociable effects of punishment and reward on motor learning. *Nat. Neurosci.* **18**, 597–602 (2015).

67. A. C. Bostan, P. L. Strick, The basal ganglia and the cerebellum: nodes in an integrated network. *Nat. Rev. Neurosci.* **19**, 338–350 (2018).

68. M. J. Wagner, T. H. Kim, J. Savall, M. J. Schnitzer, L. Luo, Cerebellar granule cells encode the expectation of reward. *Nature* **544**, 96–100 (2017).

69. W. Heffley, *et al.*, Coordinated cerebellar climbing fiber activity signals learned sensorimotor predictions. *Nat. Neurosci.* **21**, 1431–1441 (2018).

70. D. Kostadinov, M. Beau, M. Blanco-Pozo, M. Häusser, Predictive and reactive reward signals conveyed by climbing fiber inputs to cerebellar Purkinje cells. *Nat. Neurosci.* **22**, 950–962 (2019).

71. N. Larry, M. Yarkoni, A. Lixenberg, M. Joshua, Cerebellar climbing fibers encode expected reward size. *Elife* **8** (2019).

72. A. M. Haith, D. M. Huberdeau, J. W. Krakauer, The influence of movement preparation time on the expression of visuomotor learning and savings. *J. Neurosci.* **35**, 5109–5117 (2015).

73. J. O'Keefe, J. Dostrovsky, The hippocampus as a spatial map. Preliminary evidence from unit activity in the freely-moving rat. *Brain Research* **34**, 171–175 (1971).

74. T. Hafting, M. Fyhn, S. Molden, M.-B. Moser, E. I. Moser, Microstructure of a spatial map in the entorhinal cortex. *Nature* **436**, 801–806 (2005).

75. N. J. Killian, M. J. Jutras, E. A. Buffalo, A map of visual space in the primate entorhinal cortex. *Nature* **491**, 761–764 (2012).

76. N. J. Killian, S. M. Potter, E. A. Buffalo, Saccade direction encoding in the primate entorhinal cortex during visual exploration. *Proc. Natl. Acad. Sci. U. S. A.* **112**, 15743–15748 (2015).

77. J. B. Julian, A. T. Keinath, G. Frazzetta, R. A. Epstein, Human entorhinal cortex represents visual space using a boundary-anchored grid. *Nat. Neurosci.* **21**, 191–194 (2018).

78. M. Nau, T. Navarro Schröder, J. L. S. Bellmund, C. F. Doeller, Hexadirectional coding of visual space in human entorhinal cortex. *Nat. Neurosci.* **21**, 188–190 (2018).

79. N. Wilming, P. König, S. König, E. A. Buffalo, Entorhinal cortex receptive fields are modulated by spatial attention, even without movement. *Elife* **7** (2018).

80. J. L. S. Bellmund, L. Deuker, T. N. Schröder, C. F. Doeller, Grid-cell representations in mental simulation. *eLife* **5** (2016).

81. R. A. Epstein, E. Z. Patai, J. B. Julian, H. J. Spiers, The cognitive map in humans: spatial navigation and beyond. *Nat. Neurosci.* **20**, 1504–1513 (2017).

82. M. M. Garvert, R. J. Dolan, T. E. Behrens, A map of abstract relational knowledge in the human hippocampal-entorhinal cortex. *Elife* **6** (2017).

83. D. Schiller, *et al.*, Memory and Space: Towards an Understanding of the Cognitive Map. *J. Neurosci.* **35**, 13904–13911 (2015).

84. M. J. Chadwick, A. E. J. Jolly, D. P. Amos, D. Hassabis, H. J. Spiers, A goal direction signal in the human entorhinal/subicular region. *Curr. Biol.* **25**, 87–92 (2015).

85. J. Jacobs, *et al.*, Direct Electrical Stimulation of the Human Entorhinal Region and Hippocampus Impairs Memory. *Neuron* **92**, 983–990 (2016).

86. A. Goyal, *et al.*, Electrical Stimulation in Hippocampus and Entorhinal Cortex Impairs Spatial and Temporal Memory. *J. Neurosci.* **38**, 4471–4481 (2018).

87. J. F. Miller, *et al.*, Neural activity in human hippocampal formation reveals the spatial context of retrieved memories. *Science* **342**, 1111–1114 (2013).

88. J. F. Miller, I. Fried, N. Suthana, J. Jacobs, Repeating Spatial Activations in Human Entorhinal Cortex. *Current Biology* **25**, 1080–1085 (2015).

89. S. E. Qasim, *et al.*, Memory retrieval modulates spatial tuning of single neurons in the human entorhinal cortex. *Nat. Neurosci.* **22**, 2078–2086 (2019).

90. J. Jacobs, M. J. Kahana, A. D. Ekstrom, M. V. Mollison, I. Fried, A sense of direction in human entorhinal cortex. *Proc. Natl. Acad. Sci. U. S. A.* **107**, 6487–6492 (2010).

91. S. Kühn, J. Gallinat, Amount of lifetime video gaming is positively associated with entorhinal, hippocampal and occipital volume. *Mol. Psychiatry* **19**, 842–847 (2014).

92. M. A. Dalton, M. Hornberger, O. Piguet, Material specific lateralization of medial temporal lobe function: An fMRI investigation. *Hum. Brain Mapp.* **37**, 933–941 (2016).

93. S. N. Sotiropoulos, *et al.*, Advances in diffusion MRI acquisition and processing in the Human Connectome Project. *Neuroimage* **80**, 125–143 (2013).

94. M. J. Chadwick, H. M. Bonnici, E. A. Maguire, CA3 size predicts the precision of memory recall. *Proc. Natl. Acad. Sci. U. S. A.* **111**, 10720–10725 (2014).

95. B. Fischl, *et al.*, Whole brain segmentation: automated labeling of neuroanatomical structures in the human brain. *Neuron* **33**, 341–355 (2002).

96. B. Fischl, *et al.*, Automatically parcellating the human cerebral cortex. *Cereb. Cortex* **14**, 11–22 (2004).

97. J. E. Romero, P. Coupé, J. V. Manjón, HIPS: A new hippocampus subfield segmentation method. *Neuroimage* **163**, 286–295 (2017).

98. J. W. Krakauer, C. Ghez, M. F. Ghilardi, Adaptation to visuomotor transformations: consolidation, interference, and forgetting. *J. Neurosci.* **25**, 473–478 (2005).